FISEVIER

Contents lists available at ScienceDirect

Palaeogeography, Palaeoclimatology, Palaeoecology

journal homepage: www.elsevier.com/locate/palaeo





Last Interglacial coastal hydroclimate variability in Bermuda revealed by clumped isotope oyster sclerochronology

Lillian Minnebo^a, Ian Winkelstern^{a,*}, Jade Zhang^b, Sierra Petersen^b

- ^a Geology Department, Grand Valley State University, Allendale, MI, USA
- ^b Department of Earth and Environmental Sciences, University of Michigan, Ann Arbor, MI, USA

ARTICLE INFO

Editor: M Elliot

Keywords: Sclerochronology Clumped isotopes Amino acid racemization Bermuda Last Interglacial Oyster

ABSTRACT

The islands of Bermuda preserve carbonates from several glacial and interglacial intervals with demonstrated potential for reconstructing past North Atlantic climate. Here, we describe new clumped and conventional stable isotope data from *Dendostrea* (oyster) shells collected from a Last Interglacial / Marine Isotope Stage 5e (MIS 5e) deposit. Interpretation of these and past data is supported by new amino acid racemization age dating results from nine localities around Bermuda.

We find that the fossil oyster population on Verrill Island (within the present Great Sound of Bermuda) records MIS 5e temperatures and water $\delta^{18}O$ values that are similar to modern. These data contrast with the much cooler temperatures and lighter reconstructed water $\delta^{18}O$ values reconstructed for sites on the southern shore. This contrast may in part be due to timing, with the Verrill Island deposit plausibly representing an earlier and warmer portion of MIS 5e. The data also reflect meaningful, highly local differences in environment, with modern Great Sound shells perhaps living in partially restricted waters buffered from cooler and groundwater-influenced conditions along the South Shore. The mobility of *Cittarium pica* marine snails used in previous work likely also introduces exaggerated variability in those cases. Critically, incorporation of clumped isotope data across multiple sites and genera enables an understanding of Bermudian MIS 5e climate that would be meaningfully different if given data from only one site. We seek to illustrate both the complexities and potential of working with clumped isotope paleoclimate data from coastal deposits.

1. Introduction

1.1. Last Interglacial climate

The Last Interglacial Period, specifically Marine Isotope Stage 5e (MIS 5e; $\sim\!129\text{--}116$ ka), was broadly a time of similar or slightly warmer climate conditions relative to today. As temperatures warmed, glacial ice melted and eventually raised global sea level to $\sim\!6$ m higher (Dutton et al., 2015), and global average temperatures were approximately 1–2 °C warmer than preindustrial conditions (CLIMAP Project Members et al., 1984; Turney and Jones, 2010; Otto-Bliesner et al., 2013). As the most recent interval of warmer-than-present climate, the geologic record of the Last Interglacial is more intact than other interglacials (Dutton and Lambeck, 2012), making it possible to study it at higher spatial and temporal resolution. Indeed, two separate sea level rise intervals have been proposed to be resolvable within the interglacial (Kopp et al., 2009). While this past warm period is not directly

comparable to modern climate conditions due to differences including orbital parameters, it can perhaps serve as a partial analog to near-future climate change (e.g., Hoffman et al., 2017).

In the North Atlantic Ocean, time-slice proxy data from sediment cores indicate sea surface conditions were not uniformly warmer during MIS 5e, with cooler-than-modern conditions in the Central Atlantic and Caribbean, but warmer-than-modern conditions in the northern North Atlantic and Nordic Seas (CLIMAP Project Members et al., 1984; Turney and Jones, 2010; Otto-Bliesner et al., 2013; Capron et al., 2014). Situated between these areas, climate records from the islands of Bermuda can provide a unique perspective on Last Interglacial climate and can help define the 'boundary' between regions experiencing different impacts.

1.2. Geology and age dating in Bermuda

The modern islands of Bermuda are primarily made up of Pleistocene

E-mail address: winkelsi@gvsu.edu (I. Winkelstern).

^{*} Corresponding author.

carbonate rocks and paleosols covering an extinct volcanic pinnacle (Land et al., 1967). These carbonates include shoreface, foreshore, and aeolian facies from multiple sea level highstands (representing interglacials). There is broad agreement that MIS 5a and 5e are present in Bermuda as the Southampton Formation and Rocky Bay Formation, that MIS 9 is present as the Town Hill Formation, and that other rarely exposed deposits likely date to MIS 11 or older (Vacher et al., 1989; Muhs et al., 2002; Hearty, 2002; Rowe et al., 2014; Hearty and Tormey, 2017). Disagreement persists about the age of the intervening Belmont Formation. Hearty (2002) argues this unit combines with the Rocky Bay Formation to represent MIS 5e, while Rowe et al. (2014) argue it is temporally distinct and represents MIS 7, in agreement with initial mapping by Vacher et al. (1989). Here we follow the stratigraphic framework of Rowe et al. (2014), though acknowledge that our data do not directly refute the younger Belmont age of Hearty (2002).

Available geochemical dating of the above formations underpin stratigraphic interpretations and include both U-series dates from corals (Harmon et al., 1983; Muhs et al., 2002; Rowe et al., 2014) and amino acid racemization (AAR) data from land snails, whole-rock samples, and bivalve shells (Harmon et al., 1983; Hearty et al., 1992; Hearty, 2002; Fig. 1). Similarity between deposits of different ages, along with erosion, isolated deposition, and minor displacement along faults has made it challenging to extend interpretations from dated outcrops to other (even nearby) undated localities (Rowe et al., 2014). This complexity motivated our efforts to obtain new geochemical ages for our study sites (described below) and several other undated localities. While U—Th dates from coral fossils can provide absolute ages, here we apply AAR dating because of its ability to provide at least relative ages for deposits lacking suitable coral material.

AAR dating relies on the decay of amino acids in an organism (here, mollusks) to record the time since death. A predictable transition of levorotatory to dextrorotatory amino acids (more generally, the A/I ratio) is the primary measurement (Miller and Clarke, 2007). While AAR dating can be applied as an absolute dating technique in some cases

(Bada and Protsch, 1973), uncertainty around the duration and magnitude of warmth experienced by samples is a limiting factor (e.g., Hearty, 2002; Miller and Clarke, 2007). By linking AAR dates and absolute U-series dates at a subset of localities within a study region, a regional calibration between AAR ratios and absolute ages can be created and applied to other nearby sites where absolute ages are not present.

In Bermuda, Hearty et al. (1992) identified several distinct aminozones defined by specific ranges of A/I data and linked to stratigraphy. Of relevance here are their Aminozone C, with values ranging from 0.36 to 0.47; Aminozone E, with values ranging from 0.51 to 0.62; and Aminozone F, with values ranging from 0.66 to 0.72. In Bermuda Aminozones C, E, and F correlate with MIS 5a (Southampton Formation), MIS 5e (Rocky Bay Formation), and MIS 7 (Belmont Formation), respectively. (Though we note again that the age of the Belmont Formation is interpreted as an older phase of MIS 5 by Hearty (2002)). These A/I ratio ranges can then be used to assign individual outcrops to associated marine isotope stages. We presume that the whole island (~25 km long) has the same temperature history with respect to its effect on the rate of amino acid racemization.

1.3. Last Interglacial climate in Bermuda

Isotopic paleothermometry methods were recently applied to mollusks from the well-dated sites of Grape Bay and Rocky Bay (Hearty et al., 1992; Muhs et al., 2002) in order to reconstruct MIS 5e ocean temperatures around Bermuda (Winkelstern et al., 2017; Zhang et al., 2021). Mollusks are routinely used in geochemical and paleoclimate applications, as they can record and preserve temperature and water chemistry (e.g., δ^{18} O_{water}) during calcification of the shell (e.g., Wanamaker et al., 2011; Schöne and Surge, 2012; Huyghe et al., 2022).

Using marine gastropod shells of the species *Cittarium pica*, Winkelstern et al. (2017) reported MIS 5e Bermuda SSTs significantly cooler than modern. This was particularly true of the Grape Bay fossil locality

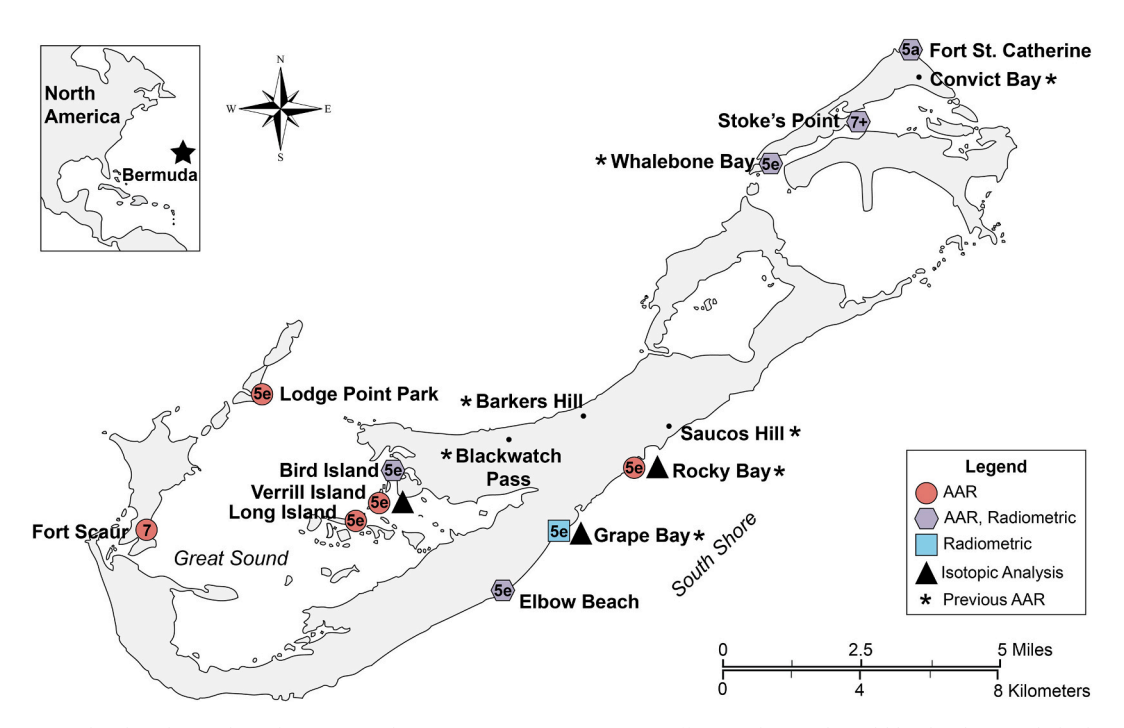


Fig. 1. Map of outcrops dated in this study with Amino Acid Racemization (AAR). Previous efforts at the purple and blue localities include the amino acid racemization work of Harmon et al. (1983), Hearty et al. (1992), and Hearty (2002), and the U/Th radiometric dating of Harmon et al. (1983), Muhs et al. (2002), and Rowe et al. (2014). The red outcrops were not previously dated. Previous MIS 5e localities with AAR dating where we did not sample for this study are also indicated. Details of specific horizons sampled in this study can be found in the Supplemental Information. Sample locations of shells used for stable isotope analysis in this study or previously are indicated with black triangle. (For interpretation of the references to colour in this figure legend, the reader is referred to the web version of this article.)

(Fig. 1), where MIS 5e shells recorded very cold (~10 °C cooler) and relatively fresh ($\delta^{18} O_{water} = \sim -1$ % VSMOW) waters. This led the authors to hypothesize that meltwater from Greenland reaching Bermuda was a plausible explanation for these cool temperatures and depleted seawater isotopic conditions. However, after Zhang et al. (2021) reanalyzed these data using updated clumped isotope methodologies and combined them with new MIS 5e and modern analyses, the magnitude of the apparent cooling and seawater depletion was reduced, negating the need to call on long-distance travel of Greenland meltwater. Zhang et al. (2021) instead found evidence in modern waters and fossil shells pointing towards local submarine groundwater discharge as a source of isotopically-depleted water, based in part on a high degree of $\delta^{18}O_{water}$ variability observed in modern waters collected along the south shore.

The totality of MIS 5e paleoclimate studied on Bermuda has been focused on fossil mollusks from the south shore sites of Grape Bay and Rocky Bay (Winkelstern et al., 2017; Zhang et al., 2021), mainly because they are some of the most reliably dated sites (Muhs et al., 2002). Yet, Zhang et al. (2021) showed that Grape Bay in particular may be unique in its susceptibility to submarine groundwater discharge. Further study is warranted on other local MIS 5e sites to determine whether the cold MIS 5e conditions are consistent across the island. The potential for species-specific paleoenvironmental biases (e.g., preferred water depth; Kirby et al., 1998; Schöne and Surge, 2012) also motivates our efforts to diversify MIS 5e proxy data across genera and localities.

Because of the challenges in assessing the age of a given exposure in Bermuda (e.g., discontinuous deposition), we sought to better constrain a set of outcrop ages with new data. Here, we apply AAR dating to four new and five previously studied sites in Bermuda. We identify potential localities that could record a different MIS 5e paleoenvironment than the groundwater-influenced south shore sites Grape Bay and Rocky Bay. We then apply high resolution stable isotopes (δ^{18} O) and clumped isotope measurements (Δ_{47}) to mollusk shells from Verrill Island in the Great Sound and compare these with published results from Grape Bay

and Rocky Bay along the south shore (Fig. 1). Unlike previous studies focusing on the gastropod *Cittarium pica* (Winkelstern et al., 2017; Zhang et al., 2021), we use the oyster species *Dendostrea frons* as proxy material. The presence of *Dendostrea* alone suggests a different paleoenvironment than the rocky south shore, where unlike the Great Sound, it has not been reported in fossil deposits or today (iNaturalist, 2023). We use these data to evaluate whether Last Interglacial climate in Bermuda was colder, as suggested by Zhang et al. (2021) and Winkelstern et al. (2017), or whether temperature anomalies relative to modern were variable across the island. This also represents the first use of *Dendostrea* as a paleoclimate archive.

2. Methods

2.1. Sample collection

We collected marine mollusk fossils from 9 outcrops around the islands (Figs. 1–3). From west to east, they are: Fort Scaur, Lodge Point Park, Long Island, Verrill Island, Bird Island, Elbow Beach, Whale Bone Bay, Stoke's Point, and Fort St. Catherine. At each of these nine exposures we focused on shell-rich horizons interpreted as shoreface deposits. As first described by Land et al. (1967), these horizons commonly lie above shallowly seawardly dipping subtidal facies with few fossils, and underlie paleosols and aeolian units deposited during subsequent glacially-driven sea level falls. A single <0.5 m horizon was sampled at each locality with the exception of Bird Island, where four separate shell-rich horizons approximately 0.5 m apart were each sampled. Stratigraphic columns, exact locations, and descriptions of each locality are available in the Supplementary Information.

Bivalve genera *Glycymeris*, *Arca*, and/or *Lucina* were collected at all sites for AAR and possible future stable isotope analysis. *Dendostrea* was sampled at Verrill Island solely for stable (including clumped) isotope work (Fig. 3). While *Dendostrea* should in principal work as an AAR proxy material as well, we did not analyze the oyster shells for AAR

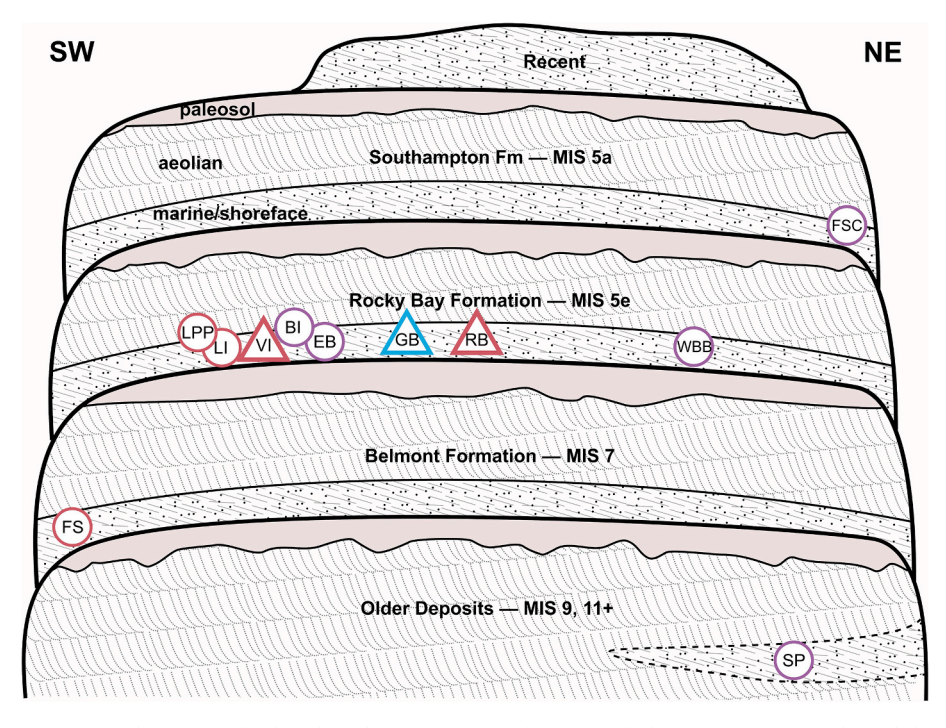


Fig. 2. Generalized schematic of Bermuda stratigraphy, based on that of Vacher et al. (1989). Thicknesses are not to scale, and these formations in reality are discontinuous across the islands. Our study sites are placed approximately along the \sim 25 km length of Bermuda along a SW to NE axis, using interpretations of data in Fig. 5 and as discussed in the text. These sites are indicated with identical symbology as in Fig. 1: Red = AAR dates only, purple = AAR and radiometric dates; blue = radiometric dates only. Triangles indicate study locations for stable isotope work. Abbreviations, from SW to NE: FS = Fort Scaur, LPP = Lodge Point Park, LI = Long Island, VI = Verrill Island, BI = Bird Island, EB = Elbow Beach, GB = Grape Bay, RB = Rocky Bay, WB = Whalebone Bay, SP = Stoke's Point, and FSC = Fort St. Catherine. (For interpretation of the references to colour in this figure legend, the reader is referred to the web version of this article.)



Fig. 3. A. *Dendostrea* bed in the shade at Verrill Island. B. More *Dendostrea* in-situ, approximately 5 m east of photo A. C. Typical bivalve preservation near base of MIS 5e layer with imbricated and rip-up clasts, here at Long Island. D. One of several shell–rich beds at Bird Island.

because 1) any genus-specific effects have not been evaluated, and more importantly 2) *Dendostrea* data from U-series dated sites do not exist like they do for *Glycymeris*, *Arca* and *Lucina*, making direct AAR comparisons impossible. About ten complete oyster shell valves were collected with eight selected for isotopic analysis. The shells were not articulated. Shell size was fairly uniform, roughly 5 cm in width and 7–15 cm in length (Figs. 3A, 4, and Supplemental Information).



Fig. 4. Sub-sampling strategy for stable isotope work on shell sample VI201. Conventional ($\delta^{18}O$ and $\delta^{13}C$) sample sites are the smaller pits, requiring <1 mg of sample powder. The three larger pits (circled) are for clumped isotope work, requiring $\sim\!15$ mg of powder. On this shell we also verified general consistency between hinge and valve cross section $\delta^{18}O$ data; pits for these samples are at the bottom right. These data and all sample photos are available in the Supplemental Information.

2.2. AAR methodology

For AAR dating, powdered samples from 47 fossil shells were analyzed at the University of Colorado Boulder Amino Acid Geochronology Laboratory. Standard methods of ion-exchange liquid chromatography and reverse-phase liquid chromatography were applied according to Wehmiller and Miller (2000). The data are reported as A/I ratios for the D-alloisoleucine/L-isoleucine amino acids. We measured A/I ratios for three genera of shells: Glycymeris, Lucina, and Arca (all data available in the Supplementary Information). To enable direct comparison with Hearty et al. (1992) results, we applied identical species-specific adjustments to our non-Glycymeris data. These result in a "Glycymeris equivalent" A/I ratio, with Arca values multiplied by 1.31 and Lucina values multiplied by 0.72. Hearty et al. (1992) also analyzed Brachiodontes and Chama shells, with their A/I ratios multiplied by 0.82 and 0.77, respectively, though we did not measure any example of these two genera. Henceforth referenced A/I values will use these adjusted values (Table 1). As discussed below, sites dated both here and in Hearty et al. (1992) show that the different AAR datasets are approximately equivalent when these species-specific adjustments are made.

As is common in AAR-based studies (e.g., Wehmiller, 2013), we base our interpretations primarily on the mean adjusted A/I value of all samples from each locality. Of the nine sites in our study, five of them have been previously dated by U—Th dating: Whalebone Bay (Harmon et al., 1983), Stoke's Point (Harmon et al., 1983), Fort St. Catherine (Muhs et al., 2002; Harmon et al., 1983), Lodge Point Park (Harmon et al., 1983), as well as perhaps Bird Island (Harmon et al., 1983, but likely a different outcrop – see below). Whalebone Bay was also previously dating using AAR (Hearty et al., 1992). We use the existing

Table 1
Amino acid racemization data, reported as the D-alloisoleucine/L-isoleucine ratio, here the A/I ratio. The species adjusted A/I ratio adds values specified in Hearty et al. (1992) to the *Lucina* and *Arca* A/I values, enabling direct comparison with their results. The four values with * were excluded from mean values and interpretation because they were outliers (2) or species identification was not conclusive (2).

Location	Species	A/I ratio	Species adjusted A/ I ratio	Mean	SE
Fort Scaur	Glycymeris	0.634	-		
		0.707	-	0.652	0.023
	Lucina	0.852	0.613		
v 1 . D	Lucina	0.670	0.482		
Lodge Point Park		0.789 0.835	0.568 0.601	0.516	0.037
		0.533	0.411		
	Glycymeris	0.560	-		
Long Island	GlyCyllielis	0.214*	0.154*	0.523	0.021
Long Island	Lucina	0.675	0.486	0.020	0.021
		0.565	-		
	Glycymeris	0.653	_		
Verrill Island	Grycymens	0.633	_		
Verrill Island		0.790	0.568	0.614	0.015
	Lucina	0.842	0.606		
	Zucina	0.918	0.661		
		0.538	_		
		0.653	_		
		0.549	_		
		0.188	-		
	Glycymeris	0.602	-		
		0.583	-		
		0.473	-		
		0.248	-		
Bird Island		0.448	-	0.529	0.020
Dira ionina		0.751	0.541	0.023	0.020
		0.482	0.347		
		0.673	0.485		
		0.775	0.558		
	Lucina	0.894	0.643		
		0.699	0.503		
		0.916	0.660		
		0.544	0.392		
		0.680	0.489		
Elbary Danah	Lucina	0.735	0.529	0.510	0.010
Elbow Beach	Lucina	0.680 0.745	0.490 0.536	0.518	0.012
	Lucina	0.743	0.628		
Whale Bone	Lucina	0.780*	-		
Bay	Unknown	0.759*	_	0.671	0.021
	Arca	0.545	0.714		
	Glycymeris	0.909	-		
Stoke's Point		0.858	_		
		0.804	_	0.844	0.019
	Lucina	0.746*	0.537*		
		1.120	0.806		
	Lucina	0.492	0.354		
Fort St.		0.559	0.402	0.378	0.030
Catherine		0.382	0.275		

absolute dates, established A/I ratio ranges for aminozones C to F (Hearty et al., 1992), and stratigraphic context to assign our previously undated localities to marine isotope stages (Fig. 5). We are not attempting to assign absolute ages based on the AAR data.

2.3. Paleoclimate shell sampling and preservation

We analyzed eight *Dendostrea* shells from Verrill Island for their isotopic composition to reconstruct paleotemperatures. These were bisected to reveal dark and light growth layers. Rather than target the hinge of each shell (as in Huyghe et al. (2019), for example) we subsampled the main inner (prismatic) layer of the valve cross sections. This was done because 1) the larger area enabled us to better avoid bored and potentially altered areas on some shells, and 2) it also enabled higher resolution of clumped isotope samples, which require much more

material than conventional analyses. An exception to this is the smaller shell VI 203, where a single clumped isotope sample was taken across the entire hinge area, which we presume averages conditions during all shell growth. Both shell hinge and valve are expected to record approximately the same environmental conditions in mollusks (Huyghe et al., 2019), and we found general agreement between hinge and valve $\delta^{18} O_{carb}$ values in test data from shell VI 201 (Supplemental Information Fig. S2). Exact sub-sampling locations for isotopic work are shown in Fig. 4 and in the Supplemental Information.

We milled ~ 0.1 mg carbonate samples (n=4 to 16) along the growth axes of each cross section for conventional stable isotope analysis using a low-speed Dremel tool, with each subsample roughly 2 mm apart. One to four larger (~ 5 mg) samples were also drilled from each shell for clumped isotope analysis: five oysters with 1 sample, two oysters with 2 samples per shell, and three oysters sampled 3 times each (Table 2).

Clumped sample selection locations were determined based on the conventional $\delta^{18}O_{carb}$ results (below), targeting local minima and maxima (presumed summers and winters) where applicable. From the three oysters with multiple samples, growth layers with peak $\delta^{18}O_{carb}$ values indicating seasonality of the warmest and coolest periods were chosen (see Supplemental Information for shell photos).

The oysters displayed original fine layering and coloration of the shell, suggesting a lack of overall diagenetic alteration. Sample powders were collected away from any encrusted or bored portions of the shell. Several of the <code>Dendostrea</code> were extensively bored in some portions, and so care was taken to sample away from these areas. Critically, no meaningful difference was observed in $\delta^{18}O_{carb}$ or clumped isotope values between bored shells and shells with less boring. The results themselves also suggest a lack of alteration, which we discuss in Section 3.2. Shells were collected from at or very near the surface, in original position of deposition. There is no possibility of sufficient burial to cause thermal resetting at this site.

2.4. Conventional stable isotope methods

Each conventional stable isotope sample was analyzed for $\delta^{13}C$ and $\delta^{18}O$ by a Kiel IV automated carbonate device attached to a Thermo-Finnegan MAT 253 dual inlet mass spectrometer at the Stable Isotope Laboratory at the University of Michigan. The data were standardized by comparison with NBS-18 and NBS-19, units in per mille (‰) relative to VPDB standard, with an uncertainty of $\pm 0.1\%$ for both $\delta^{13}C$ and $\delta^{18}O$.

2.5. Clumped isotope methods

The clumped isotope composition was measured in the SCIPP Lab at the University of Michigan using a Nu Perspective isotope dual-inlet ratio mass spectrometer connected to a NuCarb automated sample preparation device (described in Jones et al., 2022). Sample powders were measured a minimum of three times with results averaged. Methods used were identical to those described in O'Hora et al. (2022) for the Nu instrument. In summary, carbonate powders were dissolved in 103% phosphoric acid at 70 °C for 20 min, while CO2 produced was continually frozen in liquid nitrogen. Water was held in a - 60 °C trap while CO2 was released and purified by passing through a Porapak Q trap for 800 s at -30 °C. Our relatively large (\sim 5 mg) samples were analyzed in bellows mode (as opposed to small-sample cold finger mode). To maintain initial beam strength (80 nA) in the Nu Perspective over four blocks of twenty reference - sample cycles, bellows were continuously adjusted each cycle. Raw beam intensities of masses 44 through 49 were converted to clumped isotopic values using IUPAC (Brand) parameters (Brand et al., 2010) and the R code in Petersen et al. (2019). These values were then converted to the Intercarb Carbon Dioxide Equilibrium Scale absolute reference frame using measured Δ_{47} of the four ETH standards, as described in Bernasconi et al. (2021).

Sample mean $\Delta_{47\text{-ICDES}}$ values were converted to temperature via the ETH-standard based temperature calibration of Anderson et al. (2021).

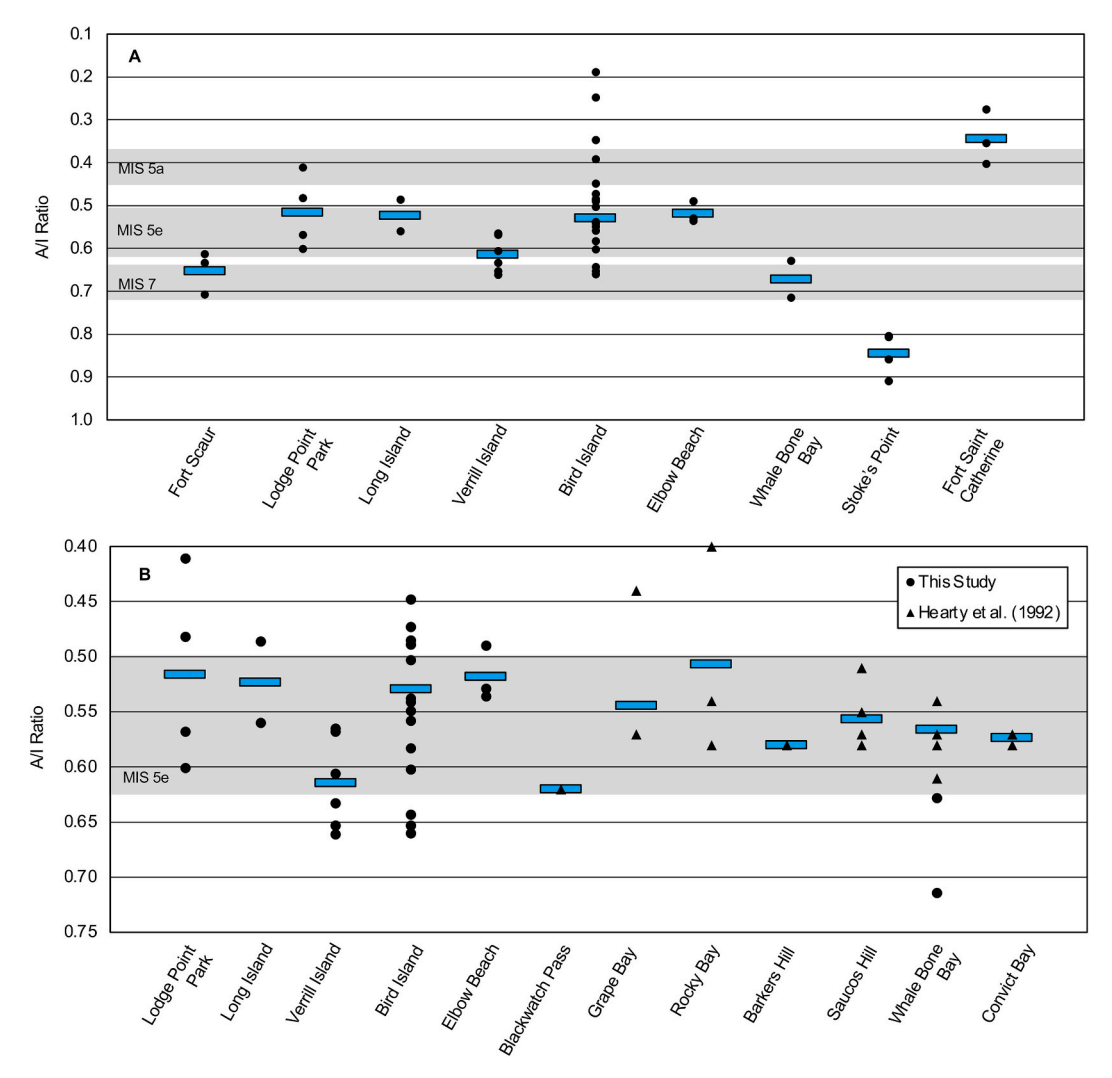


Fig. 5. A) Amino Acid Racemization (AAR) data from this study (black circles) with means indicated with blue rectangles. A/I ratios are adjusted for species-specific effects as in Hearty et al. (1992). Marine Isotope Stage (MIS) ranges are as given in Hearty et al. (1992) for Bermuda. See supplemental information for stratigraphy of sample locations. Analytical error is smaller than point size (< 0.1). B) AAR data for sites interpreted as MIS 5e from both this study and Hearty et al. (1992). Plotted means for the Hearty et al. data are weighted based on reported number of analyzed samples, as individual sample data were not reported. Each triangle represents 1–4 separate measurements, as reported (data from this study are reported as individual analyses). (For interpretation of the references to colour in this figure legend, the reader is referred to the web version of this article.)

Table 2
Descriptive statistics for conventional oxygen isotope data. All data are relative to the Vienna Pee Dee Belemnite standard (VPDB). Full data available as supplemental information.

Shell ID	n per shell	Mean δ^{18} O (‰ VPDB)	δ^{18} O range (‰)	Max δ ¹⁸ O (‰)	Min δ^{18} O (‰)
VI 201	32	-0.47 ± 0.06	1.36	0.29	-1.07
VI 202	11	-0.57 ± 0.07	0.95	-0.12	-1.07
VI 203	5	-0.47 ± 0.20	1.18	0.27	-0.91
VI 204	8	-0.86 ± 0.05	0.37	-0.74	-1.11
VI 205	3	-0.62 ± 0.15	0.59	-0.24	-0.83
VI 207	11	-0.56 ± 0.11	1.41	0.39	-1.02
VI 209-1	10	-0.25 ± 0.06	0.69	0.02	-0.66
VI 209-2	4	-0.46 ± 0.03	0.14	-0.4	-0.54

Periodic measurement of five in-house carbonate standards enable calculation of long-term reproducibility of Δ_{47} measurement as 0.018‰ at 1 standard deviation. All data have been submitted to the ClumpDB database within the EarthChem data archive.

2.6. Temperature calculations using shell $\delta^{18}O_{carb}$ and Δ_{47}

High-resolution $\delta^{18}O_{carb}$ data were converted into temperature using

the temperature fractionation for calcite and water of Kim and O'Neil (1997). Calculating temperature using $\delta^{18}O$ fractionation requires input of the $\delta^{18}O_{water}$ value in which the shell precipitated. Values for $\delta^{18}O_{water}$ were derived from Δ_{47} temperatures as follows.

First, for each clumped isotope measurement, the $\delta^{18}O_{carb}$ value acquired during that measurement is used with the calculated clumped isotope temperature to calculate a $\delta^{18}O_{water}$ value (via the mineralogically appropriate fractionation equation). For shells with a single

clumped isotope measurement, this $\delta^{18} O_{\text{water}}$ value is then used to convert each of the high-resolution $\delta^{18}O_{shell}$ measurements to a temperature as shown in Fig. 6. For shells with more than one clumped isotope measurement, the $\delta^{18}O_{water}$ value used is an average of the two closest Δ_{47} measurement locations weighted by proximity to the conventional measurement location on the shell (Fig. 6B), That is, the closer a point is to a clumped isotope measurement site, the more weight is given to that clumped isotope – based $\delta^{18}O_{water}$ value in the temperature calculation. As an example: the 5th measurement for shell VI201 is 8 mm from a measured clumped-isotope $\delta^{18}O_{water}$ value of +2.1 % VSMOW, and 17 mm from a measured clumped-isotope $\delta^{18}O_{water}$ value of +1.8~%VSMOW. Therefore, the water value used to calculate temperature (via the Kim and O'Neil (1997) equation) is 0.68*2.1 + 0.32*1.8 = 2.0 %, where 0.68 and 0.32 are the weightings for how close each clumped measurement is (with a total distance between points of 25 mm in this case).

3. Results

3.1. Age dating results and interpretations

Age interpretations for all sites are based on the data in Table 1 and Fig. 5 as well as local stratigraphic context. We identify five new MIS 5e sites (Bird Island, Elbow Beach, Lodge Point Park, Long Island, and Verrill Island), one new MIS 7 site (Four Scaur), and one pre-MIS 9 site (Stoke's Point). Where our data overlap with previous work, results are generally as expected. For example, we find an MIS 5a age for exposures at Fort St. Catherine, consistent with Harmon et al. (1983), Hearty et al. (1992), and Muhs et al. (2002). While the AAR methodology used in Hearty et al. (1992) was not identical, the data concurrence at overlapping sites indicates that the data are reasonably comparable.

With the one exception of the Whalebone Bay site (see below), data from all sites agree with our field assessments of likely ages, based largely on stratigraphic relationships (where apparent), the mapping of Vacher et al. (1989), and degree of cementation. The degree of

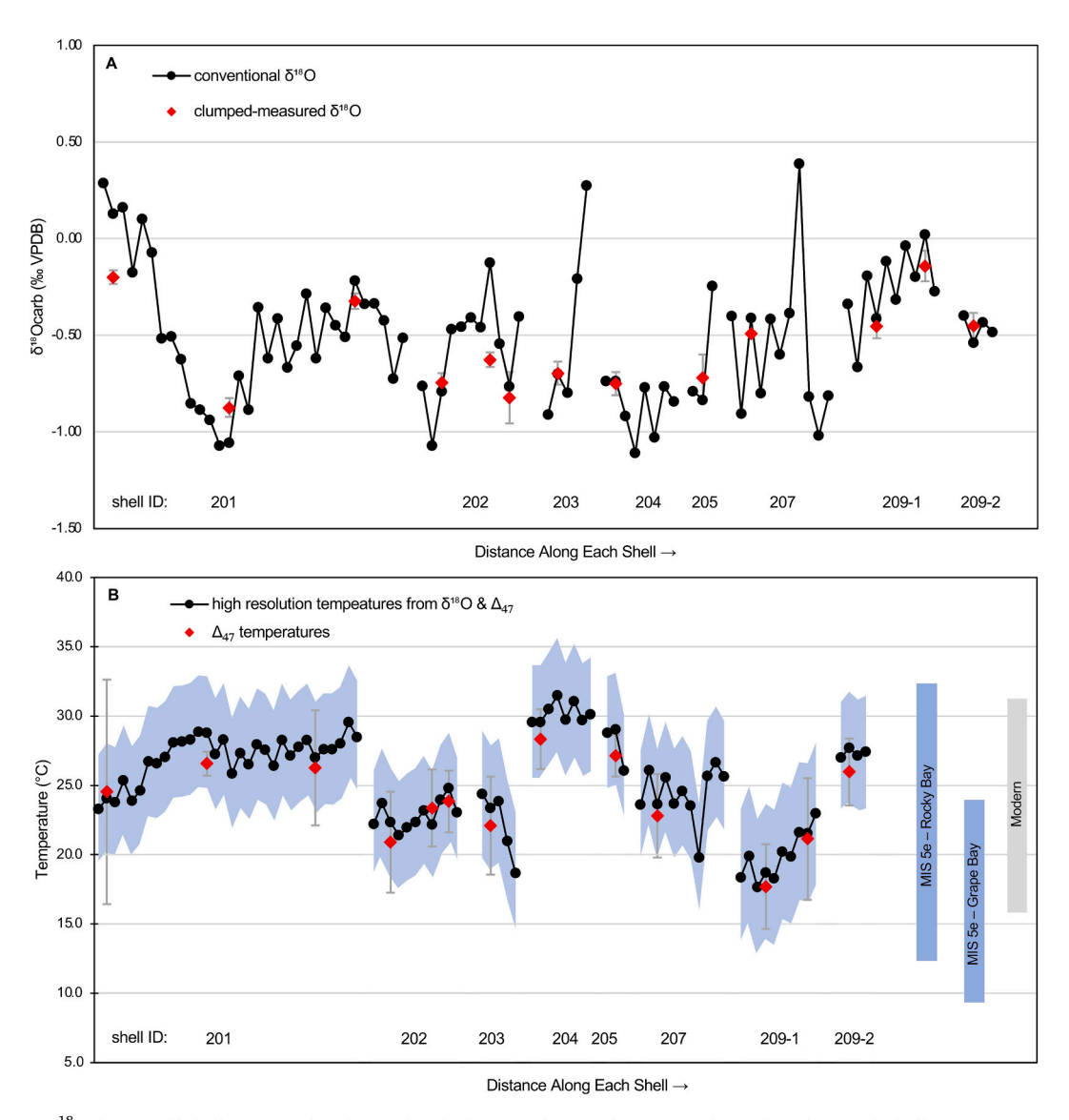


Fig. 6. A) Carbonate $\delta^{18}O$ data for all shells measured in this study. The horizontal axis indicates sample number along each shell. Error is approximately the same size as each point for conventional $\delta^{18}O$ (<0.1 ‰), and is indicated in 2 standard error bars for $\delta^{18}O$ measurements taken during clumped isotope analysis. B) Clumped isotope and carbonate $\delta^{18}O$ measurements (part A) combined to create high-resolution temperature records, as described in the text. The error envelope indicates two standard error resulting from the calculated $\delta^{18}O_{\text{water}}$ value from replicate clumped isotope measurements. The horizontal axis indicates only sample number along each shell. The blue bars indicate *Cittarium*-based temperature ranges from Zhang et al. (2021). The grey bar is the modern offshore buoy temperature range from Hervey et al. (2013). (For interpretation of the references to colour in this figure legend, the reader is referred to the web version of this article.)

cementation can often be used as a rough guide of relative age in Bermuda (Land et al., 1967), especially to distinguish between the more lithified Belmont Formation (interpreted by Rowe et al. (2014) as MIS 7) and the less lithified overlying Rocky Bay Formation (MIS 5e). This difference in lithification is observed in superposition at sites like Grape Bay and Rocky Bay. For example, we observed a high degree of lithification at Fort Scaur, which suggested an assignment of the Belmont Formation for the exposed marine layers there. This was then supported by A/I ratios in agreement with Belmont (MIS 7 age) data from other sites.

At Bird Island, shells from three stacked shell layers (Supplemental Information) yielded overlapping A/I ratio ranges, indicating that any time difference between the layers is too short to be distinguished with this technique. Harmon et al. (1983) previously reported a single younger MIS 5a U-series date from Bird Island, but there is a good chance this coral was collected from a different bed. Their locality is described as the west side of the island; our samples come from exposures at its northern tip. Further, we observed no corals in the shell beds we sampled, suggesting a different paleoenvironment. The young U-series date may also be an outlier, as the other two U-series ages from the Great Sound at Bluck's Island and Hawkins Island reported by Harmon et al. (1983) are consistent with MIS 5e. Indeed all of our data from the Great Sound of Bermuda, including Long Island and Verrill Island as well, indicate an MIS 5e age for shelly horizons outcropping above modern sea level

It is important to note, however, that Verrill Island AAR ratio values span both the MIS 5e and MIS 7 A/I ratio ranges, and it is likely that this deposit is meaningfully older (either within the MIS 5e interglacial or as part of MIS 7) than the other MIS 5e localities dated here. The Verrill Island mean AAR value of 0.61 \pm 0.04 is distinct from the \sim 0.52 mean value for Lodge Point Park, Long Island, and Elbow Beach. Still, we infer that Verrill Island shells were deposited during MIS 5e based on: 1) a mean AAR value within the MIS 5e range; 2) the mapping and interpretations of Vacher et al. (1989); 3) the general lack of cementation consistent with other MIS 5e sites; and 4) nearby (< 350 m) clearly MIS 5e AAR ratios from Long Island. Verrill Island is therefore likely representative of an earlier deposit within MIS 5e, and our paleoclimate interpretations are based on an older (but still Last Interglacial) age relative to previously studied Rocky Bay Formation deposits on the South Shore.

Interestingly, the distribution of AAR ages in the MIS 5e timespan seems to be split into older and younger groups when incorporating the full dataset of Hearty et al. (1992); (Fig. 5B). It is plausible that younger ages indicated by lower A/I ratios of roughly 0.5 at Bird Island, Elbow Beach, Lodge Point Park, and Long Island represent a younger transgression within MIS 5e. And that higher A/I ratios of roughly 0.6 at Verrill Island and the Hearty et al. (1992) sites Blackwatch Pass, Hungry Bay, and Barkers Hill indicate an older transgression within MIS 5e (and the Rocky Bay Formation). This two-transgression interpretation would be consistent with MIS 5e Atlantic sea level reconstructions that indicate two separate sea level pulses during the broader Last Interglacial high-stand (Kopp et al., 2009). The paleoclimate implications of Verrill Island being older than published data from the South Shore is discussed below (Section 4.2.3). Higher precision dating and/or field studies would be required to fully test the two-transgression hypothesis in Bermuda.

Our data from Whalebone Bay appear to suggest an MIS 7 age. However, this site has been convincingly dated to MIS 5e using U-series dating (Muhs et al., 2002), confirming previous AAR dating by Vacher and Hearty (1989). There are two likely explanations for the discrepancy: 1) the shell bed we sampled is not identical to that sampled in other studies, and represents a highly localized older deposit, or 2) it is the result of poor shell preservation. We favor the second explanation based on visible shell wear, abundant dissolution pits within shells, and friable textures. Diagenesis at Whalebone Bay was a challenge for previous researchers as well (Vacher and Hearty, 1989), who had fewer species from this site to work with compared to other sites. Due to our

low data quality from this site, we defer to the original U-series-based assignment of MIS 5e (Muhs et al., 2002) for the Whalebone Bay locality. We did not use shells from this site for paleoclimate work.

The Stoke's Point locality is clearly much older than the other sites based on available dating as well as relative stratigraphic position. Harmon et al. (1983) reported U-series ages of $\sim\!228$ to $>\!300$ ka for this site. Our AAR data agree, in that a mean A/I value of 0.844 \pm 0.06 indicates an age likely much older than MIS 7. The geology of this exposure is also markedly different from all the others, with feldspar-rich sand layers and possible weathered volcanics (See Supplemental Information). More work would be needed to understand the age and significance of this outcrop.

3.2. High resolution conventional stable isotope results

The high resolution conventional stable isotope results are found in Table 2 and Fig. 6. The eight *Dendostrea* oysters record a mean $\delta^{18}O_{carb}$ value of -0.51 ± 0.17 % (VPDB). The largest oyster (VI 201) records a gradual trend towards more negative δ^{18} O values, indicative of a potential seasonal cycle (Fig. 6). Other shell records are shorter and apparently spanned less than one year, e.g. VI 204 and VI 209-2. Shell $\delta^{18}O_{carb}$ amplitudes are quite variable, with as little as ~0.4 % as a range for VI 209–2 (with only 4 measurements) and as much as \sim 1.5 %in VI 201 and VI 207. The overall Dendostrea δ¹⁸O_{carb} range is from -1.11 to 0.39% VPDB (Fig. 6). All shell profiles are broadly consistent with each other in terms of variability around the average $\delta^{18}O_{carb}$ value. One minor exception is VI 209-1, which skews a bit more positive; this could very likely be a simple effect of small sample size, or perhaps this shell lived in slightly deeper and cooler waters. Shell VI 204 has values skewed towards more negative $\delta^{18}O_{carb}$, and thus perhaps lived in slightly shallower and warmer waters.

Interpretation of stable carbon isotopes in coastal marine mollusks is complex and hindered by the wide range of controls on shell δ^{13} C, including metabolic effects (McConnaughey and Gilliken, 2008). Our oyster δ^{13} C values varied between -0.3 and 2.7 % VPDB, with a mean of 1.9 % VPDB. (Supplemental Information Fig. S1). These values are very similar to those reported locally for MIS 5e *Cittarium Pica* in Zhang et al. (2021) and Winkelstern et al. (2017), suggesting broadly similar ambient dissolved inorganic carbon values across sites.

These results are consistent with a general lack of diagenetic alteration of our isotopic data. The isotopic data themselves support the idea that they are measurements of unaltered shell material (Section 2.3) because: 1) There is no meaningful difference between $\delta^{18}O_{\text{carb}}$ profiles or averages of highly bored and more pristine shells; 2) the visible seasonality would likely be minimized by diagenetic effects; 3) they, along with the clumped isotope data described below, do not match expected values for freshwater (diagenetic) cement compositions, like those measured by Defliese and Lohmann (2016); and most critically 4) our interpretations do not rely on any particular $\delta^{18}O_{\text{carb}}$ data point but instead consider the overall patterns in the data. Even in the case where a small number of these data do reflect some degree of alteration, our findings would not be meaningfully affected.

3.3. Clumped isotope results

The clumped isotope results are recorded in Table 3. The <code>Dendostrea</code> Δ_{47} values result in a mean temperature of $23.9\pm3.0\,^{\circ}\text{C}$, with a range of Δ_{47} temperatures between $19.1\pm1.8\,^{\circ}\text{C}$ to $28.0\pm1.3\,^{\circ}\text{C}$. These values are roughly equivalent with modern Bermuda temperatures (16–31 $^{\circ}\text{C}$; Hervey et al., 2013).

The $\delta^{18}O_{water}$ values are also shown in Table 3. The *Dendostrea* have a mean $\delta^{18}O_{water}$ value of $+1.6\pm0.6\%$, with a range of 0.9 ± 0.5 % to $+2.3\pm0.3$ % VSMOW. These data are consistent with modern seawater $\delta^{18}O$ measurements reported in Zhang et al. (2021), which range from +0.9 to +1.8% VSMOW. In particular, a single water sample taken from near Bird Island (nearby Verrill Island within the Great Sound) produced

Table 3 Clumped isotope (Δ_{47}) data for all samples. Calculated water values are reported relative to the Vienna Standard Mean Ocean Water standard (VSMOW), as calculated. Samples with multiple temperature and δ^{18} O_{water} measurements are from different locations on the shell – each measurement shown here is based on at least 3 replicate analyses. Value after the \pm symbol is one full standard error. All data are available in the supplemental information.

2.3 ± 0.5		
1.8 ± 0.1 2.1 ± 0.1		
2.1 ± 1.0		
1.3 ± 0.2		
1.4 ± 0.4 1.2 ± 0.2		
0.8 ± 0.5		
1.1 ± 0.5 1.1 ± 0.5		
2.3 ± 0.3 2.3 ± 0.3		
2.1 ± 0.2 2.1 ± 0.2		
1.5 ± 0.4 1.5 ± 0.4		
1.5 ± 0.5		
0.4 ± 0.3 0.9 ± 0.5	0.9 ± 0.5	
2.1 ± 2.1 2.1 ± 0.2		
	$\begin{array}{cccccccccccccccccccccccccccccccccccc$	

a value of +1.3 % VSMOW, in close agreement with the mean values from fossil Dendostrea.

4. Discussion

4.1. Paleoclimate conditions recorded by Dendostrea

Bivalves in general are reliable recorders of paleoclimate, and with few exceptions are thought to precipitate in approximate isotopic equilibrium with their surrounding water (Wanamaker Jr et al., 2006; Henkes et al., 2013). The Dendostrea genus in particular has not been previously used as a paleoclimate proxy, and we did not specifically evaluate the geochemistry of modern examples. However, several efforts studying stable isotopes in the Ostreidae family suggest that adult oyster growth is not subject to unique geochemical effects that would inhibit their use as a proxy. Stable isotope analyses of oyster shells with a focus on environmental reconstruction have been carried out in several studies, including Kirby et al. (1998), Surge et al. (2001), Goodwin et al. (2021), and Huyghe et al. (2022). Generally, these studies found that adult shells precipitate in equilibrium with local waters, enabling accurate (paleo)environmental reconstruction. Like all mollusk records, some inherent biases are expected as a result of several factors, including timing of shell growth during the year and water depth (Kirby et al., 1998; Marchitto et al., 2000; Schöne, 2008). Oysters in particular are fast-growing shells, with significant growth taking place during a single year, with relatively limited growth during any subsequent years (Huyghe et al., 2022). This factor likely contributed to the relatively short (\leq one year) sclerochronological records we obtained.

Most of the individual Dendostrea shells we measured show less than a year of growth in the high-resolution $\delta^{18} O_{\text{carb}}$ and temperature records (that is, no obvious seasonality). At least three Dendostrea shells do record a meaningful shift in temperature across the sampled interval (VI201: \sim 24 to \sim 30 °C; VI209–1: \sim 19 to \sim 24 °C; and VI203: \sim 25 to ~19 °C; Fig. 6B), indicating more than one season was recorded. But the generally short records are likely due to rapid growth rates and possibly limited adult growth (Huyghe et al., 2022). The short records were expected given that oyster genera Crassostrea and Magallana are known to complete most of their total growth within the first two years of life (Chávez-Villalba et al., 2005; Huyghe et al., 2019), with rate of growth dependent on highly local factors like the nearby presence of seagrass (Ricart et al., 2021). Another factor in the brief, discontinuous records may be that sampling resolution and subsample locations within each shell could have resulted in reduced apparent seasonality than what the shell actually experienced. Exact subsample locations may not have encompassed all available time preserved by a given shell, particularly on shells where care was taken to avoid potentially altered shell pits (Supplemental Information). Whatever the cause, the Dendostrea shells provide a scattered and fairly discontinuous record while still preserving

general environmental conditions that are highly likely representative of the overall environment.

Our findings further imply <code>Dendostrea</code> is a reliable recorder of climate, particularly when the generally brief geochemical 'snapshots' from each individual shell are considered together. When the records from all eight shells are combined as one population, temperatures calculated from combined $\delta^{18}O_{carb}$ and Δ_{47} measurements (range ~ 18 to $\sim 33~\rm C$; average $\sim 24~\rm ^{\circ}C$; see Section 2.5) are functionally identical to modern conditions (16–31 $^{\circ}C$; Hervey et al., 2013). Likewise, the mean $\delta^{18}O_{water}$ value of $+1.6~\pm~0.6\%$ is indistinguishable from the modern $\delta^{18}O_{water}$ measurement of +1.3~% VSMOW reported in Zhang et al. (2021) from near Bird Island ($\sim 750~m$ away within the Great Sound). Taken as a whole, the stable isotope geochemistry of this oyster population is essentially identical to what would be expected for bivalves (including <code>Dendostrea</code>) living in the shallow waters of the Great Sound today.

This suggests that the climate of the Last Interglacial in Bermuda was very similar to modern, at least during the deposition of the Verrill Island oyster bed. This is in contrast to the generally cooler conditions inferred from similar approaches at different localities on the South Shore (Zhang et al., 2021; Winkelstern et al., 2017). Indeed, slightly cooler conditions relative to modern might be expected for Bermuda based on global Last Interglacial proxy compilations (Turney and Jones, 2010; Otto-Bliesner et al., 2013; Capron et al., 2014), which describe warmer poles and cooler tropics relative to modern. Possible explanations for the differences between sites are discussed below.

4.2. Explaining hydroclimate differences between Last Interglacial sites

The warm, relatively stable conditions recorded by the Verrill Island oysters are substantially different from those reported from MIS 5e sites along the south shore at Grape Bay and Rocky Bay (Fig. 6A). There Winkelstern et al. (2017) and Zhang et al. (2021) found that Cittarium pica gastropod shells record colder, isotopically lighter, and more variable water conditions (Figs. 6B; 7A). The Grape Bay site in particular is $\sim\!1.5$ % VSMOW lighter and $\sim\!10$ °C colder, reflecting clearly different controls on shell isotopic chemistry. Because the south shore sites are only kilometers away (< 7 km) and today experience identical temperature patterns (Guishard, 2022), these marked differences in temperature, $\delta^{18}{\rm O}_{\rm water}$, and overall variability require explanation. We discuss three non-mutually-exclusive potential answers below.

4.2.1. Differences in species lifestyle

The very large variability observed in the *Cittarium* δ^{18} O_{water} data (> 5 %) but not observed in the *Dendostrea* data (~2 %) is likely in part a behavioral effect. *Cittarium pica* snails are commonly observed in tide pools, shallow waters, and also waters as much as 7 m deep (Robertson, 2003; Rosenberg, 2009). They would therefore be more likely to

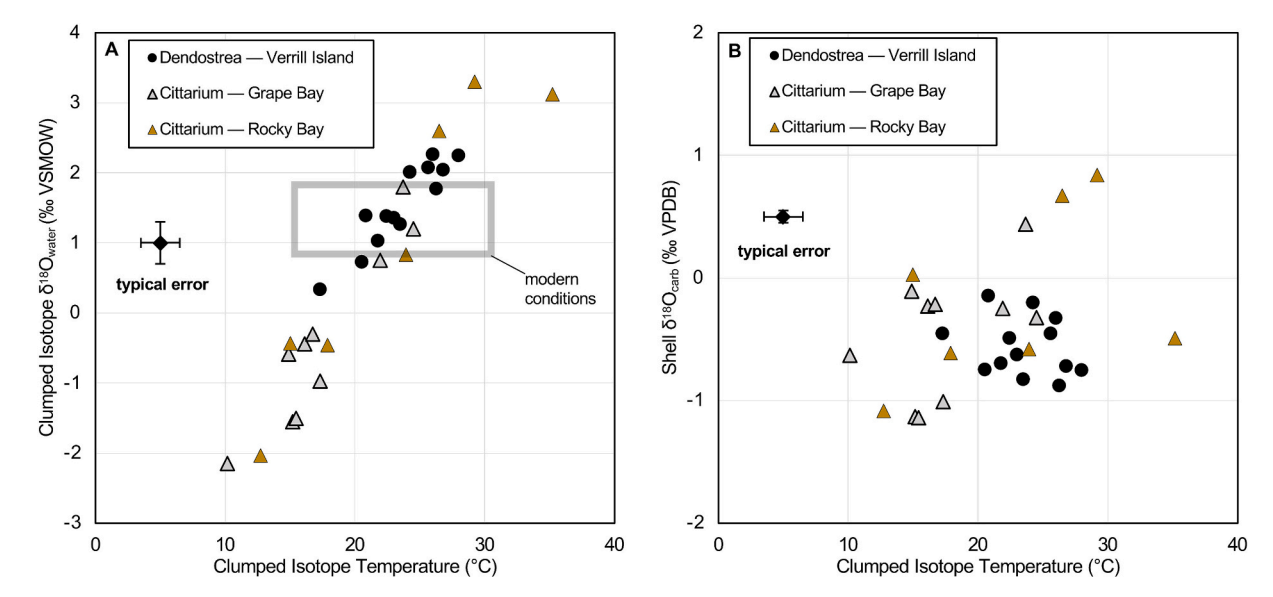


Fig. 7. A) All published clumped isotope measurements from Bermuda in this study and Zhang et al. (2021), including their reprocessed data of Winkelstern et al. (2017). Note that most shells were measured in more than one location on the shell; thus the number of data points (30) is larger than the number of shells analyzed (14; see Table 3 for data from this study). Modern temperature range is offshore buoy data from Hervey et al. (2013); the modern $\delta^{18}O_{\text{water}}$ range is from all measurements reported in Zhang et al. (2021). B) Comparison between carbonate $\delta^{18}O$ and clumped isotope temperatures from the same measurements as in part A. Mean carbonate $\delta^{18}O$ values are very similar, despite the fact that south shore *C. pica* record more variable and on average colder conditions.

experience highly localized and temporary effects (like tidal pool evaporation) as they move, relative to more stationary and permanently offshore bivalves (Olson and Hearty, 2013). Indeed, *Dendostrea* in contrast are fixed and commonly found in shallow waters, with a depth range extending upwards to low tide sea level (Rosenberg, 2009; Quigley and Hill, 2015). And today *Dendostrea* observations are constrained to the Great Sound and other sheltered areas, and have not been reported from the South Shore (iNaturalist) These oysters would be far less likely to experience variability greater than their inhabited water body. It is therefore likely that the combined *Dendostrea* temperature and $\delta^{18}{\rm O}_{\rm water}$ ranges are a more accurate measure of past seasonality, with the caveat that the short records preserved in a given shell require the combination of many shells to estimate seasonality.

Clumped isotopes in modern *Cittarium* do accurately record modern average conditions (Winkelstern et al., 2017; Zhang et al., 2021), and so the colder and lighter $\delta^{18}O_{water}$ conditions they record at on average at Rocky Bay and especially Grape Bay still require an alternative explanation. Indeed, the effect of tidal habitats would seem likely to induce a warm and heavier $\delta^{18}O_{water}$ bias in *Cittarium* relative to *Dendostrea*, if any, rather than the colder and lighter conditions observed. This mean difference is difficult to explain from species-specific effects alone, implying a real difference in environment recorded at each site.

4.2.2. Spatial variability: groundwater influence and evaporative restriction

It is very likely that highly local differences in environment affect the climate recorded by the <code>Dendostrea</code> population relative to the Rocky Bay and Grape Bay <code>Cittarium</code> population. This is because there are observable differences in hydrology between the Great Sound and the South Shore today. Local differences are particularly notable for $\delta^{18}O_{water}$; measurements by <code>Zhang</code> et al. (2021) found that Great Sound waters were essentially constant (1.2 to 1.3 ‰), while South Shore waters varied over a much wider range (0.8 to 1.8 ‰). <code>Zhang</code> et al. (2021) attributed much of this modern variation and lower $\delta^{18}O_{water}$ to local groundwater discharge, supported by proximity to the modern Devonshire Lens aquifer (<code>Vacher</code>, 1978). They showed that this discharge can result in roughly 1 ‰ VSMOW reductions in local waters in the modern, enough to explain much of the $\delta^{18}O_{water}$ difference between sites we observe

here. It is expected that all four main aquifers in Bermuda today could

also lower $\delta^{18}O_{water}$ values and increase $\delta^{18}O_{water}$ variability in relation

to changes in sea surface height, with sites near these lenses being more vulnerable to changes in $\delta^{18}O_{water}$ (Zhang et al., 2021). Meaningful differences in past aquifer size and porosity mean that Last Interglacial hydrogeology would not be identical, but it would have been sufficient to induce the location-based differences we observe (Zhang et al., 2021).

The more muted variability at Verrill island, then, would imply a lack of groundwater effects in Great Sound during MIS 5e, as seems to be the case today (Zhang et al., 2021). The ~ 1.5 % difference in $\delta^{18}O_{water}$ observed between Great Sound fossils and Grape Bay fossils could also in part be attributed to slight evaporative restriction of waters in the Great Sound relative to the more open South Shore. Last Interglacial geography was likely somewhat similar to today (though with less exposed land; Land et al., 1967), and so MIS 5e Great Sound sites could plausibly have experienced a modest relative degree of lagoonal restriction as is true today. Such an environment would be expected to correlate with increased temperatures due to reduced mixing in shallow waters (e.g., Newton and Mudge, 2003), as well as elevated $\delta^{18}O_{water}$ due to evaporation (Rohling, 2013). As such our Verrill Island record should be considered a potentially slightly warm-biased record, implying that overall conditions in Bermuda during MIS 5e were at least similar to or possibly even cooler than today. We do not think this location-related warm bias is large (if any), because of the marked similarity to modern conditions in both recorded temperature and $\delta^{18}O_{water}$.

4.2.3. Temporal variability: multiple MIS 5e high stands?

The modeling of Kopp et al. (2009) suggested that two separate major transgressions (and subsequent regressions) occurred worldwide during MIS 5e. Dating and sedimentological evidence for this has been reported in a few places in the western North Atlantic, including San Salvador, The Bahamas (Chen et al., 1991; Skrivanek et al., 2018). In Bermuda, this idea was part of the reasoning of Hearty (2002) to assign the Belmont Formation to MIS 5e, rather than MIS 7. While Rowe et al. (2014) make a clear case for the Belmont to retain its original MIS 7 age (of Vacher et al., 1989), they did not specifically rule out the existence of multiple transgressive events within the MIS 5e Rocky Bay formation. Age differences were also suggested as an explanation for the significant differences in hydroclimate between the Rocky Bay and Grape Bay sites in Winkelstern et al. (2017), though not necessarily because of separate peaks in sea level. Indeed, a steady increase in western North Atlantic

sea level during MIS 5e followed by a rapid drop was described by Dyer et al. (2021). In either case, based on available age dating (and the paleoclimate data themselves) it seems likely that temporal differences help explain the different conditions found at Verrill Island and along the South Shore.

We do not believe that our amino-acid based dating, along with that of Hearty et al. (1992), and the available U—Th data (Harmon et al., 1983; Muhs et al., 2002) are sufficiently precise to conclusively define separate transgressions in Bermuda during the \sim 20 kyr span of MIS 5e. But the clear variability in mean MIS 5e AAR ages (Section 3.1; Fig. 5B) suggests it is at least possible that some Last Interglacial deposits in Bermuda are thousands of years older than others. The Grape Bay locality in particular is more likely to be deposited later in the interglacial than earlier, based on a U—Th range extending as late as \sim 113 ka and AAR ratios that are as low as 0.44 (Muhs et al., 2002; Hearty et al., 1992). With the relatively high AAR ratio (\sim 0.61) we measured in shells from Verrill Island, as well as the slightly lower elevation of the deposit, it is therefore plausible that the Verrill Island oysters were deposited well before shells at Grape Bay (and perhaps Rocky Bay as well) within MIS 5e. This would have meaningful effects on the paleoclimate they record.

Peak warmth during the Last Interglacial would be expected to occur before peak sea level (Oppo et al., 2006; Dyer et al., 2021). In this scenario, shells deposited earlier in the stage would be expected to record warmer conditions. Shells deposited later within the stage would instead reflect cooling, despite still higher sea levels. This basic framework fits our data, with the seemingly older oysters recording warmer conditions than the cooler and seemingly younger south shore sites (especially Grape Bay). The idea also does not require distinct transgressions; deposition across the interglacial could occur as a result of sporadic deposition during transgression or regression during one or multiple individual sea level rise events.

Fully testing the idea that climate in Bermuda cooled during MIS 5e across discontinuous outcrops would require both more precise age dating and elevation data (including some accounting for vertical and/or tectonic movement; Rowe et al., 2014). Intra-outcrop variability could be another promising approach. For example bivalves at Bird Island (also in the Great Sound) were deposited in discrete superimposed layers and may record a geochemical record of environmental changes across interglacial time.

In summary, warmer and more positive $\delta^{18}O_{water}$ conditions recorded by Verrill Island oysters relative to published South Shore data are likely the result of multiple factors. Species lifestyles and highly local environmental effects logically play some role. But perhaps most intriguing is the possibility that discrete deposits record either earlier or later MIS 5e time in Bermuda, and that the earlier deposits may record a warmer climate than the later deposits. Future work on these questions could help better constrain the timing and duration of peak Last Interglacial warmth in Bermuda.

4.3. Relevance to other coastal paleoclimate work

Beyond the specific interpretations of the paleoclimate data, our findings also further illustrate the importance of clumped isotopes in allowing for two-dimensional analysis across temperature and $\delta^{18}O_{water}$. For example, an investigation of only shell carbonate $\delta^{18}O$ would not have found major differences between the Dendostrea and Cittarium data. Even at Grape Bay (which recorded markedly cooler conditions), mean shell $\delta^{18}O_{carb}$ values ranged from about -0.4 to +0.3 % VPDB (Winkelstern et al., 2017), while the Verrill Island mean shell $\delta^{18}O_{carb}$ ranged from about -0.9 to +0.2 % VPDB (Fig. 6B). The values of course are not identical, but the $\sim \! 10\,^{\circ} C$ colder mean temperature at Grape Bay was in effect hidden by simultaneously $\sim \! 1.5\,$ % lower $\delta^{18}O_{water}$ values. The ability to measure independently via clumped isotopes therefore reveals meaningful variability across a small geographic area (and across perhaps a few thousand years).

This meaningful difference between sites no more than ~5 km apart illustrates the challenge of evaluating paleoclimate in coastal regions, and the importance of obtaining proxy data from multiple environments where possible. Oxygen isotopic variability in modern coastal marine waters is not very well understood (examples include Schmidt et al., 1999; Venancio et al., 2014), implying that studying coastal isotopic variability in the geologic past requires high temporal and spatial resolution (in the form of multiple localities). Having multiple genera enables multiple perspectives as well; for example Dendostrea on their own record little inter-annual variability, and the mobility of Cittarium likely causes the wider (and exaggerated) variability they record. Further isotopic work on the Lucina and Glycymeris shells used for AAR analyses in this study would be one way to further assess the ecologic effects of shell proxy data. Fully unraveling the time, space, and ecologic variables discussed here ultimately requires more work on each. But the Dendostrea data illustrate that Last Interglacial conditions in Bermuda in at least one time and location were very similar to today, and therefore that local paleoclimate is more complex than being simply cooler than modern throughout the interval.

5. Conclusions

Here we have contributed new age dating and MIS 5e paleoclimate data for the islands of Bermuda. Our new AAR data support previous assessments of outcrop age across Bermuda, and help support our interpretation that the Verrill Island site studied here is a Last Interglacial deposit. In combination with previous work, these ages also indicate the possibility of multiple transgressions within MIS 5e in Bermuda, or at least discontinuous episodes of deposition across the interval.

The stable isotope geochemistry of *Dendostrea* from the modern Great Sound of Bermuda is essentially as would be expected for mollusks living there today. These relatively warm and stable conditions are in contrast with past work on *Cittarium* from the South Shore of Bermuda, which showed colder temperatures and lower marine $\delta^{18}O_{\text{water}}$. We consider these hydroclimate differences to be the result of differences in: 1) how oysters and top shells live; 2) the degree of open marine conditions and coastal groundwater input; and 3) time of deposition, with the warmer Verrill Island shells seemingly being deposited earlier. At the very least, the like-modern conditions recorded by these *Dendostrea* show that warmer-than-expected conditions occurred in Bermuda during the Last Interglacial.

CRediT authorship contribution statement

Lillian Minnebo: Formal analysis, Investigation, Visualization, Writing – original draft, Writing – review & editing. Ian Winkelstern: Conceptualization, Data curation, Formal analysis, Funding acquisition, Investigation, Methodology, Project administration, Supervision, Visualization, Writing – original draft, Writing – review & editing. Jade Zhang: Investigation, Methodology, Writing – original draft, Writing – review & editing. Sierra Petersen: Conceptualization, Funding acquisition, Investigation, Methodology, Supervision, Writing – original draft, Writing – review & editing.

Declaration of competing interest

The authors declare that they have no known competing financial interests or personal relationships that could have appeared to influence the work reported in this paper.

Data availability

All data are available as attached supplemental information

Acknowledgements

We thank Lora Wingate and Ashling Neary at the University of Michigan Stable & Clumped Isotope Laboratory for isotopic analysis and Chris Florian of the University of Colorado Amino Acid Geochronology Lab for amino acid analyses. Dr. Mark Rowe shared knowledge about local geology and assisted with fieldwork. This work was supported by the undergraduate Student Summer Scholar Program at Grand Valley State University and NSF grant #1903389.

Appendix A. Supplementary data

Supplementary data to this article can be found online at https://doi.org/10.1016/j.palaeo.2024.112195.

References

- Anderson, N.T., Kelson, J.R., Kele, S., Daëron, M., Bonifacie, M., Horita, J., Mackey, T.J., John, C.M., Kluge, T., Petschnig, P., Jost, A.B., Huntington, K.W., Bernasconi, S.M., Bergmann, K.D., 2021. A unified clumped isotope thermometer calibration (0.5–1,100°C) using carbonate-based standardization. Geophys. Res. Lett. 48 (7) https://doi.org/10.1029/2020g1092069.
- Bada, J.L., Protsch, R., 1973. Racemization reaction of aspartic acid and its use in dating fossil bones. Proc. Natl. Acad. Sci. 70 (5), 1331–1334. https://doi.org/10.1073/ pnas 70 5 1331
- Bernasconi, S.M., Daëron, M., Bergmann, K.D., Bonifacie, M., Meckler, A.N., Affek, H.P., Anderson, N., Bajnai, D., Barkan, E., Beverly, E., Blamart, D., Burgener, L., Calmels, D., Chaduteau, C., Clog, M., Davidheiser-Kroll, B., Davies, A., Dux, F., Eiler, J., Ziegler, M., 2021. InterCarb: a community effort to improve interlaboratory standardization of the carbonate clumped isotope thermometer using carbonate standards. Geochem. Geophys. Geosyst. 22 (5) https://doi.org/10.1029/2020gc009588.
- Brand, W.A., Assonov, S.S., Coplen, T.B., 2010. Correction for the 17O interference in δ(13c) measurements when analyzing CO2 with stable isotope mass spectrometry (IUPAC technical report). Pure Appl. Chem. 82 (8), 1719–1733. https://doi.org/10.1351/pac-rep-09-01-05.
- Capron, E., Govin, A., Stone, E.J., Masson-Delmotte, V., Mulitza, S., Otto-Bliesner, B., Rasmussen, T.L., Sime, L.C., Waelbroeck, C., Wolff, E.W., 2014. Temporal and spatial structure of multi-millennial temperature changes at high latitudes during the last interglacial. Quat. Sci. Rev. 103, 116–133. https://doi.org/10.1016/j. guascirev. 2014.08.018
- Chávez-Villalba, J., López-Tapia, M., Mazón-Suástegui, J., Robles-Mungaray, M., 2005. Growth of the oyster Crassostrea corteziensis (Herlein, 1951) in Sonora, Mexico. Aquac. Res. 36 (14), 1337–1344. https://doi.org/10.1111/j.1365-2109.2005.01345. x.
- Chen, J.H., Curran, H.A., White, B., Wasserburg, G.J., 1991. Precise chronology of the last interglacial period: 234U 230Th data from fossil coral reefs in the Bahamas. Geol. Soc. Am. Bull. 103, 82–97. https://doi.org/10.1130/0016-7606(1991) 103<0082;PCOTLI>2.3.CO:2.
- CLIMAP Project Members, Cline, R.M., Hays, J.D., Prell, W.L., Ruddiman, W.F., Moore, T. C., Kipp, N.G., Molfino, B.E., Denton, G.H., Hughes, T.J., Balsam, W.L., Brunner, C. A., Duplessy, J.-C., Esmay, A.G., Fastook, J.L., Imbrie, J., Keigwin, L.D., Kellogg, T. B., McIntyre, A., Matthews, R.K., Thompson, P.R., 1984. The last interglacial ocean. Quat. Res. 21 (2), 123–224. https://doi.org/10.1016/0033-5894(84)90098-x.
- Defliese, W., Lohmann, K., 2016. Evaluation of meteoric calcite cements as a proxy material for mass-47 clumped isotope thermometry. Geochim. Cosmochim. Acta 173, 126–141. https://doi.org/10.1016/j.gca.2015.10.022.
- Dutton, A., Lambeck, K., 2012. Ice volume and sea level during the last interglacial. Science 337 (6091), 216–219. https://doi.org/10.1126/science.1205749.
- Dutton, A., Carlson, A.E., Long, A.J., Milne, G.A., Clark, P.U., DeConto, R., Horton, B.P., Rahmstorf, S., Raymo, M.E., 2015. Sea-level rise due to polar ice-sheet mass loss during past warm periods. Science 349 (6244). https://doi.org/10.1126/science. aaa4019
- Dyer, B., Austermann, J., D'Andrea, W.J., Creel, R.C., Sandstrom, M.R., Cashman, M., Rovere, A., Raymo, M.E., 2021. Sea-level trends across the Bahamas constrain peak last interglacial ice melt. PNAS 118, 33. https://doi.org/10.1073/pnas.2026839118.
- Goodwin, D.H., Gillikin, D.P., Jorn, E.N., Fratian, M.C., Wanamaker, A.D., 2021. Comparing contemporary biogeochemical archives from *Mercenaria Mercenaria* and *Crassostrea virginica*: insights on paleoenvironmental reconstructions. Palaeogeogr. Palaeoclimatol. Palaeoecol. 562, 110110 https://doi.org/10.1016/j. palaeo.2020.110110.
- Guishard, M. (Ed.), 2022. Climate Change and Bermuda Part 1 Science and Physical Hazards. Bermuda Institute of Ocean Sciences (BIOS).
- Harmon, R.S., Mitterer, R.M., Kriausakul, N., Land, L.S., Schwarcz, H.P., Garrett, P., Larson, G.J., Leonard Vacher, H., Rowe, M., 1983. U-series and amino-acid racemization geochronology of Bermuda: implications for eustatic sea-level fluctuation over the past 250,000 years. Palaeogeogr. Palaeoclimatol. Palaeoecol. 44 (1-2), 41-70. https://doi.org/10.1016/0031-0182(83)90004-4.
- Hearty, P.J., 2002. Revision of the late pleistocene stratigraphy of Bermuda. Sediment. Geol. 153 (1–2), 1–21. https://doi.org/10.1016/s0037-0738(02)00261-0.

- Hearty, P.J., Tormey, B.R., 2017. Sea-level change and superstorms; geologic evidence from the last interglacial (MIS 5e) in the Bahamas and Bermuda offers ominous prospects for a warming Earth. Mar. Geol. 390, 347–365. https://doi.org/10.1016/j. margep. 2017.05.009
- Hearty, P.J., Vacher, H.L., Mitterer, R.M., 1992. Aminostratigraphy and ages of pleistocene limestones of Bermuda. Geol. Soc. Am. Bull. 104 (4), 471–480. https:// doi.org/10.1130/0016-7606(1992)104<0471:aaaopl>2.3.co;2.
- Henkes, G.A., Passey, B.H., Wanamaker, A.D., Grossman, E.L., Ambrose, W.G., Carroll, M.L., 2013. Carbonate clumped isotope compositions of modern marine mollusk and brachiopod shells. Geochim. Cosmochim. Acta 106, 307–325. https://doi.org/10.1016/j.gca.2012.12.020.
- Hervey, R.V., US DOC; NOAA; NWS; National Data Buoy Center, 2013. Meteorological and Oceanographic Data Collected from the National Data Buoy Center Coastal-Marine Automated Network (C-MAN) and Moored (Weather) Buoys During 2013-07 (NODC Accession 0111971) Version 1.1. National Oceanographic Data Center, NOAA. Dataset.
- Hoffman, J.S., Clark, P.U., Parnell, A.C., He, F., 2017. Regional and global sea-surface temperatures during the last interglaciation. Science 355 (6322), 276–279. https://doi.org/10.1126/science.aai8464.
- Huyghe, D., de Rafelis, M., Ropert, M., Mouchi, V., Emmanuel, L., Renard, M., Lartaud, F., 2019. New insights into oyster high-resolution hinge growth patters. Mar. Biol. 166 (48) https://doi.org/10.1007/s00227-019-3496-2.
- Huyghe, D., Daëron, M., de Rafelis, M., Blamart, D., Sébilo, M., Paulet, Y.-M., Lartaud, F., 2022. Clumped isotopes in modern marine bivalves. Geochim. Cosmochim. Acta 316, 41–58. https://doi.org/10.1016/j.gca.2021.09.019.
- iNaturalist, 2023. Research-Grade Frond Oyster Observations by User b_eddy (accessed 8–2023). Accessed at: https://www.inaturalist.org/observations/120258549.
- Jones, M.M., Petersen, S.V., Curley, A.N., 2022. A tropically hot mid-cretaceous north American western interior seaway. Geology 50 (8), 954–958. https://doi.org/ 10.1130/e49998.1.
- Kim, S.-T., O'Neil, J.R., 1997. Equilibrium and nonequilibrium oxygen isotope effects in synthetic carbonates. Geochim. Cosmochim. Acta 61 (16), 3461–3475. https://doi. org/10.1016/s0016-7037(97)00169-5.
- Kirby, M.X., Soniat, T.M., Spero, H.J., 1998. Stable isotope sclerochronology of pleistocene and recent oyster shells (*Crassostrea virginica*). PALAIOS 13 (6), 560. https://doi.org/10.2307/3515347.
- Kopp, R.E., Simons, F.J., Mitrovica, J.X., Maloof, A.C., Oppenheimer, M., 2009. Probabilistic assessment of sea level during the last interglacial stage. Nature 462 (7275), 863–867. https://doi.org/10.1038/nature08686.
- Land, L.S., Mackenzie, F.T., Gould, S.J., 1967. Pleistocene history of Bermuda. Geol. Soc. Am. Bull. 78 (8), 993. https://doi.org/10.1130/0016-7606(1967)78[993:phob]2.0. co:2.
- Marchitto, T.M., Jones, G.A., Goodfriend, G.A., Weidman, C.R., 2000. Precise temporal correlation of Holocene mollusk shells using sclerochronology. Quat. Res. 53 (2), 236–246. https://doi.org/10.1006/qres.1999.2107.
- McConnaughey, T., Gilliken, D., 2008. Carbon isotopes in mollusk shell carbonates. Geo-Mar. Lett. 28, 287–299. https://doi.org/10.1007/s00367-008-0116-4.
- Miller, G.H., Clarke, S.J., 2007. Amino-acid dating. In: Encyclopedia of Quaternary Science, pp. 41–52. https://doi.org/10.1016/b0-44-452747-8/00059-4.

 Muhs, D.R., Simmons, K.R., Steinke, B., 2002. Timing and warmth of the last interglacial
- Muhs, D.R., Simmons, K.R., Steinke, B., 2002. Timing and warmth of the last interglacial period: new U-series evidence from Hawaii and Bermuda and a new fossil compilation for North America. Quat. Sci. Rev. 21, 1355–1383. https://doi.org/10.1016/S0227-3791(01)00114-7
- Newton, A., Mudge, S.M., 2003. Temperature and salinity regimes in a shallow mesotidal lagoon, the Ria Formosa, Portugal. Estuar. Coast. Shelf Sci. 57 (1–2), 73–85. https://doi.org/10.1016/S0272-7714(02)00332-3.
- O'Hora, H.E., Petersen, S.V., Vellekoop, J., Jones, M.M., Scholz, S.R., 2022. Clumpedisotope-derived climate trends leading up to the end-cretaceous mass extinction in Northwestern Europe. Clim. Past 18 (9), 1963–1982. https://doi.org/10.5194/cp-18-1963-2022
- Olson, S.L., Hearty, P.J., 2013. Periodicity of extinction and recolonization of the West Indian topshell *Cittarium pica* in the Quaternary of Bermuda. Biol. J. Linn. Soc. 110, 235–243. https://doi.org/10.1111/bij.12119.
- Oppo, D.W., McManus, J.F., Cullen, J.L., 2006. Evolution and demise of the last interglacial warmth in the subpolar North Atlantic. Quat. Sci. Rev. 25, 3268–3277. https://doi.org/10.1016/j.quascirev.2006.07.006.
- Otto-Bliesner, B.L., Rosenbloom, N., Stone, E.J., McKay, N.P., Lunt, D.J., Brady, E.C., Overpeck, J.T., 2013. How warm was the last interglacial? New model—data comparisons. Philos. Trans. R. Soc. A Math. Phys. Eng. Sci. 371 (2001), 20130097. https://doi.org/10.1098/rsta.2013.0097.
- Petersen, S.V., Defliese, W.F., Saenger, C., Daëron, M., Huntington, K.W., John, C.M., Kelson, J.R., Bernasconi, S.M., Colman, A.S., Kluge, T., Olack, G.A., Schauer, A.J., Bajnai, D., Bonifacie, M., Breitenbach, S.F., Fiebig, J., Fernandez, A.B., Henkes, G.A., Hodell, D., Winkelstern, I.Z., 2019. Effects of improved 17 O correction on interlaboratory agreement in clumped isotope calibrations, estimates of mineral-specific offsets, and temperature dependence of acid digestion fractionation. Geochem. Geophys. Geosyst. 20 (7), 3495–3519. https://doi.org/10.1029/2018.008137
- Quigley, D.T.G., Hill, R., 2015. Frond oyster (Dendostrea frons (L.)) stranded at Waterville, Co Kerry. Irish Nat. J. 34 (2), 128–129. https://www.jstor.org/stable/ 44572800
- Ricart, A., Gaylord, B., Hill, T., Sigwart, J., Shukla, P., Ward, M., Ninokawa, A., Sandford, E., 2021. Seagrass-driven changes in carbonate chemistry enhance oyster shell growth. Oecologia 196, 565–576. https://doi.org/10.1007/s00442-021-04949-0.

- Robertson, R., 2003. The edible West Indian "whelk" Cittarium pica: natural history with new observations. Proc. Acad. Natl. Sci. Phila. 153, 27–47. https://doi.org/10.1635/ 0097-3157(2003)153[0027:TEWIWC]2.0.CO;2.
- Rohling, E., 2013. Oxygen isotope composition of seawater. In: Elias, S.A. (Ed.), The Encyclopedia of Quaternary Science, 2, pp. 915–922.
- Rosenberg, G., 2009. Malacolog 4.1.1: A Database of Western Atlantic Marine Mollusca. www.malacolog.org.
- Rowe, M.P., Wainer, K.A.I., Bristow, C.S., Thomas, A.L., 2014. Anomalous MIS 7 sea level recorded on Bermuda. Quat. Sci. Rev. 90, 47–59. https://doi.org/10.1016/j. quascirev.2014.02.012.
- Schmidt, G.A., Bigg, G.R., Rohling, E.L., 1999. Global Seawater Oxygen-18 Database v1.22. https://data.giss.nasa.gov/o18data/.
- Schöne, B.R., 2008. The curse of physiology—challenges and opportunities in the interpretation of geochemical data from mollusk shells. Geo-Mar. Lett. 28 (5–6), 269–285. https://doi.org/10.1007/s00367-008-0114-6.
- Schöne, B., Surge, D.M., 2012. Treatise online no. 46: part N, revised, volume 1, chapter 14: bivalve sclerochronology and geochemistry. In: Treatise Online. https://doi.org/ 10.17161/to.v0i0.4297.
- Skrivanek, A., Li, J., Dutton, A., 2018. Relative sea-level change during the last interglacial as recorded in Bahamian fossil reefs. Quat. Sci. Rev. 200, 160–177. https://doi.org/10.1016/j.quascirev.2018.09.033.
- Surge, D., Lohmann, K.C., Dettman, D.L., 2001. Controls on isotopic chemistry of the American oyster, Crassostrea virginica: implications for growth patterns. Palaeogeogr. Palaeoclimatol. Palaeoecol. 172 (3–4), 283–296. https://doi.org/10.1016/s0031-0182(01)00303-0
- Turney, C.S.M., Jones, R.T., 2010. Does the Agulhas current amplify global temperatures during super-interglacials? J. Quat. Sci. 25 (6), 839–843. https://doi.org/10.1002/igs_1423
- Vacher, H.L., 1978. Hydrogeology of Bermuda significance of an across-the-island variation in permeability. J. Hydrol. 39 (3–4), 207–226. https://doi.org/10.1016/ 0022-1694(78)90001-x.

- Vacher, H.L., Hearty, P., 1989. History of stage 5 sea level in Bermuda: review with new evidence of a brief rise to present sea level during substage 5A. Quat. Sci. Rev. 8 (2), 159–168. https://doi.org/10.1016/0277-3791(89)90004-8.
- Vacher, H.L., Rowe, M.P., Garrett, P., 1989. The Geologic Map of Bermuda. The Ministry of Works and Engineering, The Bermuda Government.
- Venancio, I.M., Belem, A.L., dos Santos, T.H., do Zucchi, M., Azevedo, A.E., Capilla, R., Albuquerque, A.L., 2014. Influence of continental shelf processes in the water mass balance and productivity from stable isotope data and on the Southeastern Brazilian coast. J. Mar. Syst. 139, 241–247. https://doi.org/10.1016/j.jmarsys.2014.06.009.
- Wanamaker Jr., A.D., Kreutz, K.J., Borns Jr., H.W., Introne, D.S., Feindel, S., Barber, B.J., 2006. An aquaculture-based method for calibrated bivalve isotope paleothermometry. Geochem. Geophys. Geosyst. 7 (9) https://doi.org/10.1029/ 2005.0001189
- Wanamaker, A.D., Hetzinger, S., Halfar, J., 2011. Reconstructing mid- to high-latitude marine climate and ocean variability using bivalves, coralline algae, and marine sediment cores from the Northern Hemisphere. Palaeogeogr. Palaeoclimatol. Palaeoecol. 302 (1–2), 1–9. https://doi.org/10.1016/j.palaeo.2010.12.024.
- Wehmiller, J., 2013. Interlaboratory comparison of amino acid enantiometric ratios in Pleistocene fossils. Quaternary Geochronol. 16, 173–182. https://doi.org/10.1016/j. quageo.2012.08.007.
- Wehmiller, J.F., Miller, G.H., 2000. Aminostratigraphic dating methods in quaternary geology. In: AGU Reference Shelf, pp. 187–222. https://doi.org/10.1029/rf004p0187.
- Winkelstern, I.Z., Rowe, M.P., Lohmann, K.C., Defliese, W.F., Petersen, S.V., Brewer, A. W., 2017. Meltwater pulse recorded in last interglacial mollusk shells from Bermuda. Paleoceanography 32 (2), 132–145. https://doi.org/10.1002/2016pa003014.
- Zhang, J.Z., Petersen, S.V., Winkelstern, I.Z., Lohmann, K.C., 2021. Seasonally variable aquifer discharge and cooler climate in Bermuda during the last interglacial revealed by subannual clumped isotope analysis. Paleoceanogr. Paleoclimatol. 36 (6) https:// doi.org/10.1029/2020pa004145.